Signal-space projection method for separating MEG or EEG into components

Article *in* Medical & Biological Engineering & Computing · April 1997

DOI: 10.1007/BF02534144 · Source: PubMed

2 authors:

Mikko Uusitalo
Nokia
84 PUBLICATIONS **3,727** CITATIONS
SEE PROFILE

Risto J Ilmoniemi
Aalto University
423 PUBLICATIONS **25,368** CITATIONS
SEE PROFILE

Communication

Signal-space projection method for separating MEG or EEG into components

M. A. Uusitalo[1] **R. J. Ilmoniemi**[2]

[1]Brain Research Unit, Low Temperature Laboratory, Helsinki University of Technology, 02150 Espoo, Finland
[2]BioMag Laboratory, Medical Engineering Centre, Helsinki University Central Hospital, 00290 Helsinki, Finland

Keywords—*Brain mapping, Electroencephalography, Equivalent current dipole, Functional imaging, Inverse problem, Magnetoencephalography, Signal-space projection, Source analysis.*

Med. & Biol. Eng. & Comput., 1997, **35**, 135–140

1 Introduction

CURRENTS INSIDE a conducting body can be estimated by measuring the magnetic and/or the electric field at multiple locations outside and then constructing a solution to the inverse problem, i.e. determining a current configuration that could have produced the measured field. Unfortunately, there is no unique solution to this problem (HELMHOLTZ, 1853) unless restricting assumptions are made.

The minimum-norm estimate (HÄMÄLÄINEN and ILMONIEMI, 1994) provides a solution with the smallest expected overall error when minimum *a priori* information about the source distribution is available. Other methods to estimate a continuous current distribution producing the measured signals have been studied (PASCUAL-MARQUI *et al.*, 1994; WANG *et al.*, 1995; GORODNITSKY, *et al.*, 1995). A different approach is to divide the brain activity into discrete components such as current dipoles (SCHERG, 1990; MOSHER *et al.*, 1992). Here we widen this approach into arbitrary current configurations.

In our signal-space projection (SSP) method, the signals measured by d sensors are considered to form a time-varying vector in a d-dimensional signal space. The component vectors, i.e. the signals caused by the different neuronal sources, have different and fixed orientations in the signal space. In other words, each source has a distinct and stable field pattern.

All the current configurations producing the same measured field pattern are indistinguishable on the basis of the field: they have the same vector direction in the signal space and thus belong to the same equivalence class of current configurations (TESCHE *et al.*, 1995*a*). The angle in the signal space between vectors representing different equivalence classes, e.g. between component vectors, is a measure of similarity of the equivalence classes in signal space and a way to characterise the separability of sources. The cosine of this angle has previously been used as a numerical characterisation of the difference between topographical distributions (DESMEDT and CHALKLIN, 1989).

If the direction of at least one of the component vectors forming the measured multi-channel signal can be determined from the data, or is known otherwise, SSP can be used to simplify subsequent analysis. For example, if an early deflection in an evoked response is produced by one source, and the rest of the response is a mixture of signals from this and other sources, SSP can separate the data into two parts so that the early source contributes only to one part. In general, the signals are divided into two orthogonal parts: $s_{\parallel}$, including the time-varying contribution from sources with known signal-space directions; and $s_{\perp}$, including the rest of the signals. Both $s_{\parallel}$ and $s_{\perp}$ can then be analysed separately in more detail. By analysing $s_{\perp}$, we can detect activity originally masked by $s_{\parallel}$. On the other hand, the sources included in $s_{\parallel}$ are seen with an enhanced signal-to-noise ratio. By forward modelling of sources in selected patches of cortex, it is possible to form a spatial filter that selectively passes only the signals that may have been generated by currents in the given patches. If the subspace defined by artefacts can be determined, the artefact-free $s_{\perp}$ can be analysed.

In SSP, in contrast to PCA (HARRIS, 1975; MAIER *et al.*, 1987) and other analysis methods (GRUMMICH *et al.*, 1991; KOLES *et al.*, 1990; KOLES, 1991; SOONG and KOLES, 1995; BESA*), the source decomposition does not depend on the orthogonality of source components or the availability of source or conductivity models. No conductivity or source models are needed if the component vectors are estimated directly from the measured signals. This is useful when no source estimation is needed, e.g. when artefacts or somatomotor activity in a cognitive study must be filtered out. The angles between the components provide an easy and illustrative way to characterise the linear dependence between the components and thus the separability of sources.

The concept of signal space in MEG was introduced previously (ILMONIEMI, 1981; ILMONIEMI and WILLIAMSON,

First received 20 May and in final form 19 September 1996.

* BESA approach, Brain Electric Source Analysis, M. Scherg, Neuro Scan, Herndon, Virginia

1987; ILMONIEMI *et al.*, 1987). The SSP method, invented previously (ILMONIEMI, 1992; 1993), was first applied to MEG signals by Miettinen (MIETTINEN, 1992). We performed a systematic analysis and evaluation of the method (UUSITALO, 1993; UUSITALO *et al.* 1994). Tesche *et al.* described a practical application of the method, and Hämäläinen presented a mathematical summary (TESCHE *et al.*, 1995*a*; HÄMÄLÄINEN, 1995). Huotilainen *et al.* used the method to identify and remove eye-blink artefacts, and Jousmäki and Hari used it to remove cardiac artects (HUOTILAINEN *et al.*, 1993; JOUSMÄKI and HARI, 1996). Berg and Scherg presented a related method to remove eye artefacts (BERG and SCHERG, 1994). Examples of the use of SSP have been provided by Tesche *et al.* and Salmelin *et al.*, and SSP has also been demonstrated to characterise the local oscillatory content of spontaneous cortical activity during mental imagery (TESCHE *et al.*, 1995*a*; *b*; SALMELIN *et al.*, 1995).

This work, largely based on our previous work (UUSITALO, 1993; UUSITALO *et al.*, 1994), presents the mathematical basis of SSP, relates it to other comparable methods and analyses the accuracy of the method.

2 SSP method

2.1 *Basic concepts*

We consider the outcome of a measurement of the electromagnetic field with a d-channel device as a time-dependent d-component signal vector $\boldsymbol{m}(t)$. The set of all values of $\boldsymbol{m}$ forms the d-dimensional signal space $\mathcal{F}_d$.

Here, a source is defined as a set of current elements whose amplitudes behave identically as a function of time, and a component vector is defined as the signal vector caused by one source. As the relative amplitudes of the current elements forming a source do not change, a component vector has a fixed orientation in the signal space. In other words, each source corresponds to a constant output pattern whose amplitude changes with time.

The measured signal vector is a sum of M component vectors and noise

$$\boldsymbol{m}(t) = \sum_{i=1}^{M} a_i(t)\boldsymbol{s}_i + \boldsymbol{n}(t) = \boldsymbol{S}\boldsymbol{a}(t) + \boldsymbol{n}(t) \tag{1}$$

where $\boldsymbol{s}_i$ are linearly independent unit-length component vectors defined by the geometrical configuration of the sources; $\boldsymbol{a}(t)$ is their time-varying amplitude; and $\boldsymbol{n}(t)$ is noise. The matrix $\boldsymbol{S} = (\boldsymbol{s}_1, \boldsymbol{s}_2, \ldots, \boldsymbol{s}_M)$ is independent of time.

The component vectors are often estimated one at a time. Then new component vectors $\boldsymbol{s}_i$ that depend linearly on the others are not accepted, because they would represent a linear combination of the activity of the others.

The projection operators $\boldsymbol{P}_\parallel$ and $\boldsymbol{P}_\perp$ are the tools for carrying out SSP, i.e. for dividing the signals into contributions from different sets of sources. The contribution from selected sources $1, \ldots, k$ $(1 \leqslant k < M)$ can be separated by dividing the signals $\boldsymbol{m}$ into two parts: $\boldsymbol{s}_\parallel$, belonging to the subspace spanned by the component vectors $1, \ldots, k$; and $\boldsymbol{s}_\perp$, which cannot be produced by any linear combination of sources included in matrix $\boldsymbol{K} = (\boldsymbol{s}_1, \boldsymbol{s}_2, \ldots, \boldsymbol{s}_k)$

$$\boldsymbol{s}_\parallel = \boldsymbol{P}_\parallel \boldsymbol{m} \quad \boldsymbol{s}_\perp = \boldsymbol{P}_\perp \boldsymbol{m} \tag{2}$$

These operators can be computed with the help of the singular-value decomposition of the matrix $\boldsymbol{K} = \boldsymbol{U}\boldsymbol{\Lambda}\boldsymbol{V}^T$. The first k columns of $\boldsymbol{U}$ form an orthonormal basis for the column space of $\boldsymbol{K}$, and therefore

$$\boldsymbol{P}_\parallel = \boldsymbol{U}_k\boldsymbol{U}_k^T \quad \boldsymbol{P}_\perp = \boldsymbol{I} - \boldsymbol{P}_\parallel \tag{3}$$

$\boldsymbol{U}_k$ contains the first k columns of $\boldsymbol{U}$ and $\boldsymbol{I}$ is the unit matrix. The amplitudes $\boldsymbol{a}$ of the components $(\boldsymbol{s}_1, \boldsymbol{s}_2, \ldots, \boldsymbol{s}_k)$ can be estimated from

$$\hat{\boldsymbol{a}}(t) = \boldsymbol{V}\boldsymbol{\Lambda}^{-1}\boldsymbol{U}^T\boldsymbol{m}(t) \tag{4}$$

and minimise the norm $\|\boldsymbol{K}\hat{\boldsymbol{a}}(t) - \boldsymbol{m}(t)\|^2$.

2.2 *SSP method in brief*

The use of the SSP method requires that we first select k component vectors to form the matrix $\boldsymbol{K} = (\boldsymbol{s}_1, \boldsymbol{s}_2, \ldots, \boldsymbol{s}_k)$. The measured signals $\boldsymbol{m}(t)$ are then divided, according to eqn. 2, into two parts: $\boldsymbol{s}_\parallel$, including an estimate of the signals produced by the sources $1, \ldots, k$; and $\boldsymbol{s}_\perp$, including the rest. Both $\boldsymbol{s}_\parallel$ and $\boldsymbol{s}_\perp$ can be used for further analysis.

$\boldsymbol{s}_\parallel$ gives the contribution of the sources $1, \ldots, k$ with an enhanced signal-to-noise ratio. This is especially useful in the analysis of unaveraged data (TESCHE *et al.*, 1995*a*). By forming $\boldsymbol{K}$ from calculated magnetic fields produced by *ad hoc* sources, we can form a spatial filter $\boldsymbol{P}_\parallel$, passing only those signals that could have been generated by the given sources. The amplitudes of the sources $1, \ldots, k$ can be estimated according to eqn. 4.

Small unknown sources masked by the known ones can be examined in $\boldsymbol{s}_\perp$. By forming $\boldsymbol{K}$ from characterised artefacts, we can study the artefact-free $\boldsymbol{s}_\perp$. The SSP method has been reported as a tool for removing artefacts caused by eye blinks (HUOTILAINEN *et al.*, 1993), the heart (JOUSMÄKI and HARI, 1996) or by homogeneous gradients (HÄMÄLÄINEN, 1995).

2.3 *Estimation of component vectors*

Component vectors can be estimated without models directly from the measured signals $\boldsymbol{m}(t)$, if we can select a time instant t_i, when the source of interest is known to be strong compared with other components of $\boldsymbol{m}$. The selection of t_i can be based on knowledge from previous studies, on additional measurements, on the constancy of the direction of the measured signal vector, on the form of a signal, or on other additional information or assumptions. The estimate $\hat{\boldsymbol{s}}_i = \boldsymbol{m}(t_i)/\|\boldsymbol{m}(t_i)\|$ deviates from the true direction of a given source because of the presence of other sources and noise.

The estimation of a component vector can be facilitated by taking additional measurements in the presence of as few distracting sources as possible. For example, let us consider a cognitive task in which the subject responds by moving a finger. Before the task, we can measure the activity produced by the finger movement alone. This contribution can then be projected from the signals in the cognitive task.

When sources are modelled, e.g. by current dipoles, $\boldsymbol{s}_i$ can be computed from the model $\hat{\boldsymbol{s}}_i = \boldsymbol{c}(\boldsymbol{x})/\|\boldsymbol{c}(\boldsymbol{x})\|$, either by setting the model parameters $\boldsymbol{x}$ *ad hoc*, or by minimising eqn. 5. The estimate $\hat{\boldsymbol{s}}_i$ deviates from the correct unit component vector $\boldsymbol{s}_i$ owing to noise and other active sources, as well as approximations introduced by the source and conductivity models.

If the aim is to filter away the estimated contribution of certain 'unwanted' sources from given data and there is no need to model the unwanted activity, individual component vectors are not needed. Instead, the vertical columns of the matrix $\boldsymbol{K}$ can be linear combinations of component vectors, because they span the same subspace. Principal-component analysis (HARRIS, 1975) can be useful in estimating the dimensionality of the subspace spanned by the unwanted sources.

2.4 *Modelling the signals*

A current model can be used to estimate the source configuration producing the signals $s_\perp$. The model-derived signals c must be subjected to the same projection operators that were applied to the original data. Thus, for example, in least-squares minimisation, the parameters x of the model are obtained by minimising

$$\|\boldsymbol{P}_\perp \boldsymbol{m} - \boldsymbol{P}_\perp \boldsymbol{c}(x)\| \tag{5}$$

The resulting $c(x)$ need not be orthogonal to the vectors projected out by $\boldsymbol{P}_\perp$.

2.5 *Error estimates for current model parameters*

2.5.1 *Arbitrary current models:* In the following, we consider a situation in which contributions of known component vectors are first removed from $\boldsymbol{m}$ by applying $\boldsymbol{P}_\perp$. The effect of noise on current model parameters underlying an unknown component vector s_1 is then examined. The signals s_1 can be decomposed as

$$\boldsymbol{s}_1 = \boldsymbol{P}_\parallel \boldsymbol{s}_1 + \boldsymbol{P}_\perp \boldsymbol{s}_1 = \boldsymbol{s}_\parallel + \boldsymbol{s}_\perp \tag{6}$$

The angle in $\mathcal{F}$ between s_1 and $s_\parallel$ is

$$\Theta = \arccos \frac{\boldsymbol{s}_1 \cdot \boldsymbol{s}_\parallel}{\|\boldsymbol{s}_1\| \|\boldsymbol{s}_\parallel\|} \tag{7}$$

Noise causes the projected signals $\boldsymbol{P}_\perp \boldsymbol{m} = \boldsymbol{P}_\perp \boldsymbol{s}_1 + \boldsymbol{P}_\perp \boldsymbol{n}$ to deviate from the direction of the noiseless $\boldsymbol{P}_\perp \boldsymbol{s}_1$ by an angle δ. If δ is small, its effect on parameter x_i estimated from the projected data is

$$\Delta x_i = (\partial x_i / \partial \delta)\delta = \delta / k_{x,i} \tag{8}$$

where $k_{x,i} = (\partial x_i / \partial \delta)^{-1}$. For simplicity, the dependence of Δx_i on the direction of δ has been left out of the formula. When the signal-to-noise ratio (SNR) is high, $\delta \sim 1/SNR$, and

$$\Delta x_i \sim \frac{1}{SNR} \sim \frac{\sigma}{\|\boldsymbol{s}_1\| \sin \Theta} \tag{9}$$

where σ is the standard deviation of the noise in each sensor. The constant of proportionality depends on the current model and measurement geometry (see following Section).

2.5.2 *Current dipole model:* the estimated current dipole parameters x, y, z, Q_x, Q_y, and Q_z deviate from x_0, y_0, z_0, $Q_{x,0}, Q_{y,0}$ and $Q_{z,0}$ that would be obtained without noise. There is an error Δr in location, an error ΔQ in dipole moment, and an error $\Delta\Omega$ in dipole direction†. By neglecting noise parallel to $\boldsymbol{P}_\perp \boldsymbol{s}_1$,

$$\delta = \arctan \frac{\|\boldsymbol{P}_\perp \boldsymbol{n}\|}{\|\boldsymbol{P}_\perp \boldsymbol{s}_1\|} \approx \arctan \frac{\sigma\sqrt{d - d'}}{\|\boldsymbol{s}_1\| \sin \Theta}, \tag{10}$$

d' is the number of vectors included in $\boldsymbol{P}_\parallel$ and noise is assumed to be normally distributed in all channels, $n_i = N(0, \sigma)\ \forall i$. As the dimension of the affecting noise is reduced with minimising eqn. 5, it is better to use

$$\delta \approx \arctan \frac{\sigma\sqrt{p}}{\|\boldsymbol{s}_1\| \sin \Theta} \approx \frac{\sigma\sqrt{p}}{\|\boldsymbol{s}_1\| \sin \Theta} \tag{11}$$

† $\Delta Q = \sqrt{(Q_x - Q_{x,0})^2 + (Q_y - Q_{y,0})^2 + (Q_z - Q_{z,0})^2}$ and $\Delta\Omega$ is the angle between the dipoles $Q = (Q_x Q_y Q_z)^T$ and $Q_0 = (Q_{x,0} Q_{y,0} Q_{z,0})^T$. The dipole moment is denoted by Q

where p is the number of model parameters. The last approximation requires a high SNR. The estimates $\widehat{\Delta r}$, $\widehat{\Delta Q}$ and $\widehat{\Delta\Omega}$, calculated according to eqns. 8 and 11 are

$$\widehat{\Delta r} = \frac{\sqrt{p}\sigma}{k_r \|\boldsymbol{s}_1\| \sin \Theta} \tag{12}$$

$$\widehat{\Delta\Omega} = \frac{\sqrt{p}\sigma}{\|\boldsymbol{s}_1\| \sin \Theta} \tag{13}$$

$$\widehat{\Delta Q} = \frac{\sqrt{p}\|\boldsymbol{Q}\|\sigma}{\|\boldsymbol{s}_1\| \sin \Theta} \tag{14}$$

In the calculation, it was assumed that perpendicular equal-amplitude dipoles produce perpendicular signal vectors of equal length. When this is true, the angle between component vectors in the signal space is the same as the angle between the corresponding dipole directions (assuming the same dipole locations), and $k_\Omega = 1$, $k_Q = 1/\|\boldsymbol{Q}\|$. The particular measurement system determines k_r. The results of simulations (Fig. 3*d*) with the 122-sensor system Neuromag-122™ (AHONEN *et al.*, 1993) show that this assumption is approximately satisfied in practice for tangential sources. Radial dipoles in MEG analysis can be neglected, because they produce no detectable signal.

3. Angles between component vectors

The key factors affecting the accuracy of SSP are the SNR and the angles between component vectors. The separability of sources improves as the corresponding component vectors become more perpendicular. The simplest and most widely used source model is the current dipole. Therefore, we calculated angles between signal vectors produced by dipoles. The sensor array used in the calculations was like that in the Neuromag-122, shown in Fig. 1.

A reference dipole was placed in three areas (A_1, A_2 and A_3, Fig. 1), within a spherically symmetric conductor model, at distances of 5, 6, 7, 8 and 9 cm from the sphere origin O. Areas A_1 and A_2 were directly under one Neuromag-122 sensor unit. The reference dipole determined the local coordinate system (Fig. 2). A second dipole was moved in this system by changing only one parameter (ϕ, α, β, x_d, y_d or z_d) at a time. The behaviour of the angle Θ between the signal vectors of these dipoles is illustrated in Figs. 3 and 4.

Fig. 3 shows that Θ behaves quite similarly for all three reference points, as long as they are equidistant from the sensor array surface. The difference is smallest between areas A_1 and A_2 as, in these locations, the reference dipole is under the centre of one measuring sensor. The behaviour of Θ as a function of α and β is similar to the behaviour as a function of x_d and y_d, respectively.

When changing the depth z_d of the second dipole or moving it along its direction, i.e. varying y_d, Θ grows markedly slower than when the second dipole is moved sideways (x_d). This is in agreement with the fact that the localisation of a dipole is most accurate sideways, and about equally accurate in depth and in the direction along the dipole (KNUUTILA *et al.*, 1993).

As seen in Fig. 3*d*, Θ differed very little from the angle between the dipole directions in areas A_1 and A_2. Thus, the assumption concerning perpendicular equal-amplitude dipoles, used in calculating the estimates in Section 2.5.2, is very good when the current dipole is directly under a pair of measurement coils. The assumption would be exactly true if there were no other measuring coils.

™ trademark

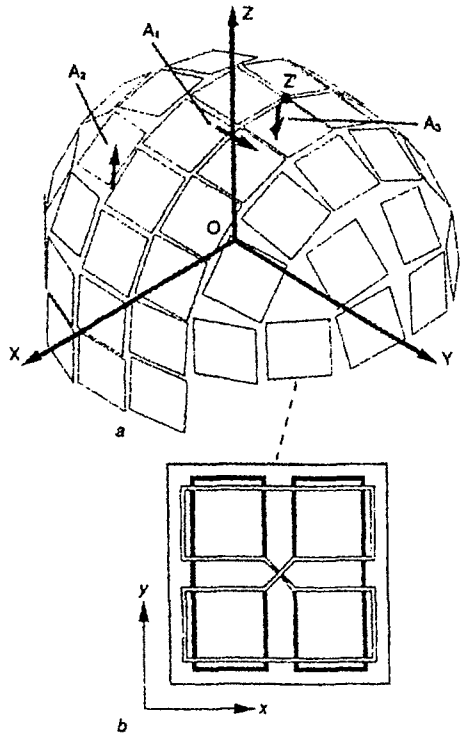

Fig. 1 *(a) Test dipoles under array of sensor units of Neuromag-122 instrument; dipoles are on positive Z-axis, pointing towards positive Y-direction in area A_1; on negative Y-axis pointing along positive Z-direction in area A_2; dipoles in area A_3 are obtained from those in area A_1 by rotating Z-axis to pass from origin O to point Z'; (b) gradient components of magnetic field $\partial B_z/\partial x$ and $\partial B_z/\partial y$ are measured by each sensor unit containing two orthogonal figure-of-eight coils*

When the dipoles were moved with respect to each other at different distances from the sphere model origin O in area A_1, Θ grew faster on the surface of the skull (Fig. 4). The shallower the dipoles were, the more a change in their location changed the direction of the signal vector in the signal space. The angle Θ behaved approximately linearly as a function of ϕ at all depths.

4 Accuracy of SSP and error estimates

Simulations were carried out to test the accuracy of the SSP method as well as the derived error-estimate formulas. The sum of the signals produced by the reference dipole, a second dipole and noise were calculated for all locations and orientations illustrated in Figs. 3 and 4. In some cases, a third dipole was added. The contributions of the second and third dipoles

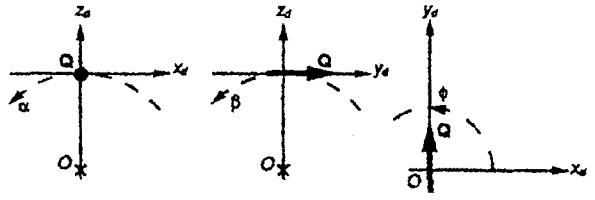

Fig. 2 *Local co-ordinate system fixed to reference dipole Q (bold arrow); co-ordinates are marked by x_d, y_d and z_d; α and β = displacement sideways and along direction of dipole, keeping distance from origin O constant; current dipole Q remains directed along tangent of dashed circle as α or β is changed; ϕ = orientation in plane of dipole; for reference dipole Q shown, $\alpha = 0°$, $\beta = 0°$ and $\phi = 90°$*

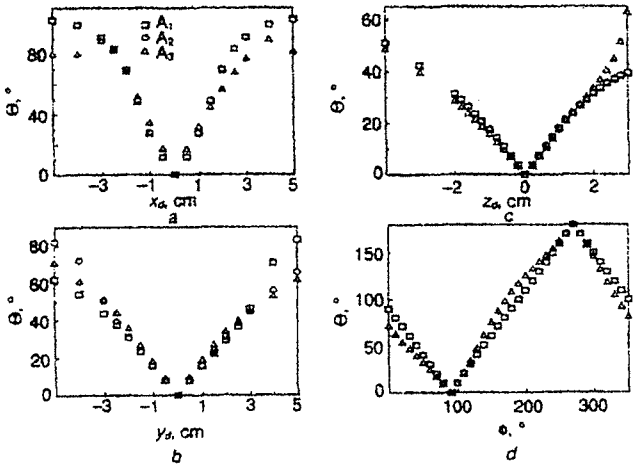

Fig. 3 *Angle Θ between signal vectors of reference and second dipoles as functions of varied co-ordinate (in local co-ordinate system, Fig. 2), when* reference *dipole is in A_1, A_2, or A_3, 7 cm from origin of sphere model*

were filtered away from the signals by the projection operator. The estimated parameters of the dipole determined by minimising eqn. 5 were compared with those of the true reference dipole.

4.1 *Method*

The locations r_i and the directions $Q_i/\|Q_i\|$ of the second and third dipoles were assumed to be known. The dipole amplitude was 10 nA m, which is typical for evoked responses.

The passband was assumed to be 0–100 Hz and the signals were assumed to be an average of 100 responses. Noise in all channels was assumed to be uncorrelated and normally distributed, $n_i = N(0, \sigma)$ for all i, with $\sigma = [500\ \text{fT}/(\text{m}\sqrt{\text{Hz}})] \cdot (\sqrt{100\ \text{Hz}}/\sqrt{100}) = 500\ \text{fT m}^{-1}$.

A projection operator was formed according to eqn. 2. The dipole parameter estimates were calculated as averages from 100 simulations. As an initial guess, a dipole at a distance of about 1 cm and 1 nA m from the real one was used.

4.2 *Results*

The errors Δr, ΔQ and $\Delta\Omega$ from the simulations are plotted in Fig. 5 as functions of Θ. The solid line is of the form $C_0/\sin\Theta$, according to the calculated error estimates eqns. 12–14. The results were similar when a third dipole was present.

The agreement between the simulated results and the calculated estimate certify that the model parameter errors depend linearly on $(\sin\Theta)^{-1}$. The angle Θ between compo-

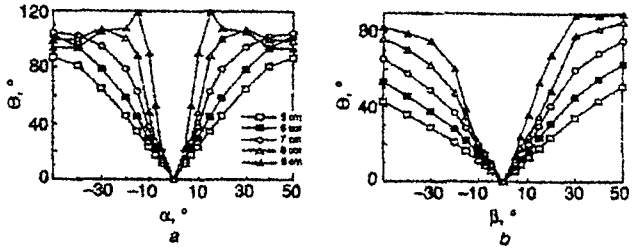

Fig. 4 *Angle Θ between signal vectors of reference and second dipoles as function of varied co-ordinate (in local co-ordinate system, Fig. 2), when reference dipole is 5, 6, 7, 8, or 9 cm from sphere model origin in A_1*

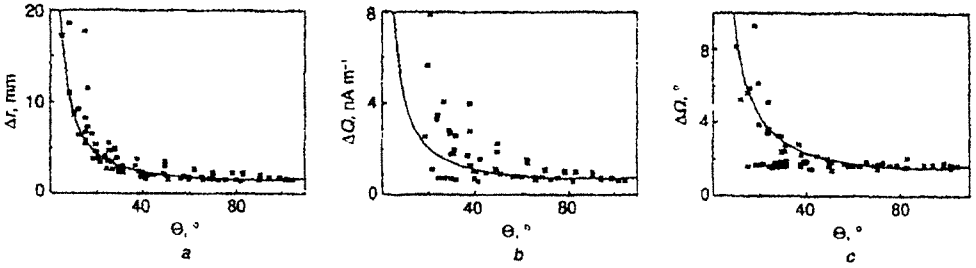

Fig. 5 *Errors (a) Δr, (b) ΔQ and (c) ΔΩ as function of Θ when dipole to be fitted (reference dipole) is in A_1, 7 cm from sphere model origin; (a)–(c) information computed from simulations during which α, β, x_d, y_d or z_d was varied; solid line is form $C_0/\sin\Theta$; C_0 has been adjusted to right order of magnitude at $\Theta = 90°$*

nent vectors determines the separability of the sources. If $\Theta = 30°$, the error in determining the source parameters is about $1/\sin 30° = 2$ times greater than when the interfering signals from the known sources do not exist. Errors grow rapidly as Θ becomes less than 30°. Thus, the limit of separability of the sources with SSP is roughly $\Theta = 30°$. Thus, in the situation illustrated in Fig. 3, the resolution is ± 1 cm in x_d and ± 2 cm in y_d and z_d.

5 Discussion

Considering MEG and EEG signals as linearly weighted sums of time-varying but spatially fixed source patterns, we constructed projection operators to divide the signals into two parts; $s_{\parallel}$, including the time-varying contribution from sources with known signal-space directions; and $s_{\perp}$, including the rest of the signals. Both parts can be separately analysed, as explained in Section 2.2. The behaviour of model error parameters for the unknown part was examined. It was found that the errors were inversely proportional to the SNR and sin Θ, where Θ is the angle between the signal produced by the modelled activity and $s_{\parallel}$. It was concluded that if $\Theta < 30°$, source localisation becomes unreliable. The behaviour of Θ was examined in particular for current dipoles recorded by the Neuromag-122™ system.

Restricting all sources to current dipoles in a known volume–conductor geometry reduces SSP to the commonly used multi-dipole approximation (SCHERG, 1990; MOSHER *et al.*, 1992). This approach applies equally to distributed and other non-dipolar sources and to situations where the conductivity structure is unknown.

In estimating the accuracy of the SSP method, the directions of the signals, and thus the locations $\boldsymbol{r}_i$ and the orientations $\boldsymbol{Q}_i/\|\boldsymbol{Q}_i\|$ of the dipoles included in the projection operator, were assumed to be known exactly. The error $\Delta\Gamma$ in knowing the exact directions in the signal space causes additional noise in the analysis. This noise is proportional to the product of $\sin(\Delta\Gamma)$ and the amplitude of the signal vector that is projected away.

The angle Θ between component vectors determines the separability of the sources. The angles between component vectors depend on the measurement geometry, but eqn. 9 and Fig. 5 are more generally applicable.

When the sources oscillate with distinct frequencies, it may be beneficial to transform the data into the frequency domain to separate the sources. The analysis of Fourier-transformed data is analogous to that of time-dependent data (LÜTKENHÖNER, 1992; TESCHE and KAJOLA, 1993; SALMELIN and HÄMÄLÄINEN, 1995). An example of this, in relation to the SSP method, is the study (TESCHE *et al.*, 1995*b*) on the local oscillatory content of spontaneous cortical activity during mental imagery.

The idea of estimating the activity in a certain area of the brain by a linear combination of signals measured outside the skull has been presented previously. Robinson and Rose called their method spatial filter imaging (SFI) and used it to create 'virtual sensors' to look at brain activity in specific areas (ROBINSON and ROSE, 1992). Ahlfors *et al.* employed linear combinations of signals, determined by the minimum-norm-estimation procedured (AHLFORS *et al.*, 1992; HÄMÄLÄINEN and ILMONIEMI, 1994), to detect unaveraged visually evoked responses. Lütkenhoner *et al.* increased the SNR of single-trial auditory evoked responses by first determining a fixed dipole on the basis of averaged data and then letting only its amplitude vary on the basis of unaveraged signals (LÜTKENHÖNER *et al.*, 1993).

When looking for components of a certain form that are not strongly correlated, the search can be automatically done using the subspace scanning method in MUSIC (MOSHER *et al.*, 1992). Here, the problems are the selection of the number of components and the suitability of the selection of the form of the components. In addition to searching for individual components, both PCA and MUSIC can be used to divide the signal space into the 'significant signal' and noise spaces. After this the 'significant signal' space can be used for further analysis, e.g. to fit dipoles (SOONG and KOLES, 1995).

Acknowledgments—The authors would like to thank K. Grönrös, M. Huotilainen, M. Hämäläinen, O. V. Lounasmaa, K. Portin, L. Narici and C. Tesche for useful comments on the manuscript, and S. Ahlfors, R. Hari, and K. Uutela for discussions.

This work was supported by the Academy of Finland, the Magnus Enhrnrooth Foundation and the Vilho, Yrjö, and Kalle Väisälä Foundation.

References

AHLFORS, S. P., ILMONIEMI, R. J., and HÄMÄLÄINEN, M. S. (1992): 'Estimates of visually evoked cortical currents,' *Electroenceph. Clin. Neurophysiol.*, **82**, pp. 225–236

AHONEN, A. I., HÄMÄLÄINEN, M. S., M. S., KAJOLA, M. J., KNUUTILA, J. E. T., LAINE, P. P., LOUNASMAA, O. V., PARKKONEN, L. T., SIMOLA, J. T., and TESCHE, C. D. (1993): '122-channel SQUID instrument for investigating the magnetic signals from the human brain,' *Physica Scripta* **T49**, pp. 198–205

BERG, P., and SCHERG, M. (1994): 'A multiple source approach to the correction of eye artifacts,' *Electroenceph. Clin. Neurophysiol.*, **90**, pp. 229–241

DESMEDT, J. E., and CHALKLIN, V. (1989): 'New method for titrating differences in scalp topographic patterns in brain evoked potential mapping,' *Ibid.*, **74**, pp. 359–366

GORODNITSKY, I. F., GEORGE, J. S., and RAO, B. D. (1995): 'Neuromagnetic source imaging with FOCUSS: a recursive weighted minimum norm algorithm,' *Ibid.* **95**, pp. 231–251

GRUMMICH, P., VIETH, J., and KOBER, H. (1991): 'Magnetic fields of the brain analysed by a multiple dipole approach using factor analysis,' *Clin. Phys. Physiol. Meas.*, **12** (Suppl. A), pp. 61–66

HÄMÄLÄINEN, M. S., and ILMONIEMI, R. J. (1994): 'Interpreting magnetic fields of the brain: minimum norm estimates,' *Med. Biol. Eng. Comput.*, **32**, pp. 35–42

HÄMÄLÄINEN, M. S. (1995): 'Functional localization based on measurements with a whole-head magnetometer system,' *Brain Topog.*, **7**, pp. 283–289

HARRIS, R. J. (1975): 'A primer of multivariate statistics' (Academic Press, New York).

HELMHOLTZ, H. *von* (1853): 'Ueber einige Gesetze der Vertheilung elektrischer Ströme in Körperlichen Leitern, mit Anwendung auf die thierisch-elektrischen Versuche,' *Ann. Phys. Chem.*, **89**, pp. 211–233, 353–377

HUOTILAINEN, M., ILMONIEMI, R. J., TIITINEN, H., LAVIKAINEN, J., ALHO, K., KAJOLA, M., SIMOLA, J., and NÄÄTÄNEN, R. (1993): 'Eye-blink removal for multichannel MEG measurements' *in* DEECKE, L., BAUMGARTNER, C., STROINK, G., and WILLIAMSON, S. J. (Eds.): Abstracts of Int. Conf. on Biomagnetism, Vienna, Austria, 14–20 August, pp. 209–210

ILMONIEMI, R. (1981): '7-channel SQUID magnetometer for brain research'. MSc Thesis, Department of Technical Physics, Helsinki University of Technology

ILMONIEMI, R. J., and WILLIAMSON, S. J. (1987): 'Analysis of the magnetic alpha rhythm in signal space,' *Soc. Neurosci. Abstr.*, **13**, p. 46

ILMONIEMI, R. J., WILLIAMSON, S. J., and HOSTETLER, W. E. (1987): 'New method for the study of spontaneous brain activity' *in* ATSUMI, K., KOTANI, M., UENO, S., KATILA, T., and WILLIAMSON, S. J. (Eds.): Biomagnetism 87 (Tokyo Denki University Press, Tokyo) pp. 182–185

ILMONIEMI, R. J. (1992): 'Method and apparatus for separating the different components of evoked response and spontaneous activity brain signals as well as signals measured from the heart. Finnish patent application 925461, 30 November

ILMONIEMI, R. J. (1993): 'Method and apparatus for separating the different components of evoked response and spontaneous activity brain signals as well as signals measured from the heart'. International patent application PCT/F193/00504, 30 November

JOUSMÄKI, V., and HARI, R. (1996): 'Cardiac artifacts in magnetoencephalogram,' *J. Clin. Neurophysiol.*, **13**, pp. 172–176

KNUUTILA, J. E. T., AHONEN, A. I., HÄMÄLÄINEN, M. S., KAJOLA, M. J., LAINE, P. P., LOUNASMAA, O. V., PARKKONEN, L. T., SIMOLA, J. T. A., and TESCHE, C. D. (1993): 'A 122-channel whole-cortex SQUID system for measuring the brain's magnetic fields,' *IEEE Trans.*, **MAG-29**, pp. 3315–3320

KOLES, Z. J., LAZAR, M. S., and ZHOU, Z. (1990): 'Spatial patterns underlying population differences in the background EEG,' *Brain Topog.*, **2**, pp. 275–284

KOLES, Z. J. (1991): 'The quantitative extraction and topographic mapping of the abnormal components in the clinical EEG,' *Electroenceph. Clin. Neurophysiol.*, **79**, pp. 440–447

LÜTKENHÖNER, B. (1992): 'Frequency-domain localization of intracerebral dipolar sources,' *Ibid.*, **82**, pp. 112–118

LÜTKENHÖNER, B., PANTEV, C., GRUNVALD, A., and MENNINGHAUS, E. (1993): 'Source-space projection of single trials of the auditory evoked field' *in* DEECKE, L., BAUMGARTNER, C., STROINK, G., and WILLIAMSON, S. J. (Eds.): Abstracts of Int. Conf. on Biomagnetism, Vienna, Austria, 14–20 August, pp. 203–204

MAIER, J., DAGNELIE, G., SPEKREIJSE, H., and VAN DIJK, B. W. (1987): 'Principal components analysis for source localization of VEPs in man,' *Vision Res.*, **27**, pp. 165–177

MIETTINEN, M. (1992): 'Magnetic measurements of visually evoked responses'. MSc Thesis, Department of Technical Physics, Helsinki University of Technology

MOSHER, J. C., LEWIS, P. S., and LEAHY, R. M. (1992): 'Multiple dipole modeling and localization from spatio-temporal MEG data,' *IEEE Trans.*, **BME-39**, pp. 541–557

PASCUAL-MARQUI, R. D., MICHEL, C. M., and LEHMANN, D. (1994): 'Low resolution electromagnetic tomography: a new method for localizing electrical activity in the brain,' *Int. J. Psychophys.*, **18**, pp. 49–65

ROBINSON, S. E., and ROSE, D. F. (1992): 'Current source image estimation by spatially filtered MEG' *in* HOKE, M., ERNÉ, S. N., OKADA, Y. C., and ROMANI, G. L. (Eds.): 'Biomagnetism: clinical aspects' (Elsevier, Amsterdam) pp. 761–765

SALMELIN, R. H., and HÄMÄLÄINEN, M. S. (1995): 'Dipole modelling of MEG rhythms in time and frequency domains,' *Brain Topog.* **7**, pp. 251–257

SALMELIN, R., HÄMÄLÄINEN, M., KAJOLA, M., and HARI, R. (1995): 'Functional segregation of movement-related rhythmic activity in the human brain,' *Neuroimage*, **2**, pp. 237–243

SCHERG, M. (1990): 'Fundamentals of dipoles source potential analysis' *in* GRANDORI, F., HOKE, M., and ROMANI, G. L. (Eds.): 'Auditory evoked magnetic fields and electric potentials' (Karger, Basel), pp. 40–69

SOONG, A. C. K., and KOLES, Z. J. (1995): 'Principal-component localization of the sources of the background EEG,' *IEEE Trans.*, **BME-42**, pp. 59–67

TESCHE, C., and KAJOLA, M. (1993): 'A comparison of the localization of spontaneous neuromagnetic activity in the frequency and time domains,' *Electroenceph. Clin. Neurophysiol.*, **87**, pp. 408–416

TESCHE, C. D., UUSITALO, M. A., ILMONIEMI, R. J., HUOTILAINEN, M., KAJOLA, M., and SALONEN, O. (1995*a*) 'Signal-space projections of MEG data characterize both distributed and well-localized neuronal sources,' *Electroenceph. Clin. Neurophysiol.*, **95**, pp. 189–200

TESCHE, C. D., UUSITALO, M. A., ILMONIEMI, R. J., and KAJOLA, M. J. (1995*b*): 'Characterizing the local oscillatory content of spontaneous cortical activity during mental imagery,' *Cogn. Brain Res.*, **2**, pp. 243–249

UUSITALO, M. A. (1993): 'Projection method in magnetoencephaolography'. MSc Thesis, Department of Technical Physics, Helsinki University of Technology

UUSITALO, M. A., ILMONIEMI, R. J., and TESCHE, C. D. (1994): 'The signal-space projection (SSP) method. Abstracts of 5th Int. Congress of Int. Society for Brain Electromagnetic Topography,' Münster, Germany, 2–6 August, p. 60

WANG, J. -Z., WILLIAMSON, S. J., and KAUFMAN, L. (1995): 'Kinetic images of neuronal activity of the human brain based on the spatio-temporal MNLS inverse: a theoretical study,' *Brain Topog.*, **7**, pp. 193–200